PHYSICAL REVIEW E **73**, 025201(R) (2006)

Experimental steady pattern formation in reaction-diffusion-advection systems

David G. Míguez,[1,*] Razvan A. Satnoianu,[2] and Alberto P. Muñuzuri[3]
[1]*Chemistry Department, Brandeis University, Waltham, Massachusetts 02454, USA*
[2]*Faculty of Actuarial Science and Statistics, Cass Business School, City University, London, United Kingdom*
[3]*Group of Complex Systems, Universidade de Santiago de Compostela, 15782 Santiago de Compostela, Spain*
(Received 26 September 2005; published 3 February 2006)

We present here experimental evidence of a mechanism of a steady-chemical pattern formation called "flow-and-diffusion structures" (FDS). Experiments were performed using the photosensitive chlorine dioxide-iodine-malonic acid reaction, where the differential diffusion can be chemically controlled. Using the analogy between an advection boundary and a moving boundary, we obtain the formation of spatially periodic steady patterns, which matches all the previously theoretical predictions for FDS patterns. Numerical simulations are also reported in agreement with the experimental results.

DOI: 10.1103/PhysRevE.73.025201 PACS number(s): 82.40.Ck, 05.45.−a, 05.65.+b, 47.54.−r

The study of pattern formation in reaction-diffusion (RD) systems is a very active area of research. In response to Turing's work [1], many studies involving chemical patterns have been recently performed. Today Turing's scenario lies at the heart of many applications attempting to explain patterns in fish skin, mammalian coat markings, phyllotaxis, and so on [2–8].

Recent studies have revealed the existence of unexplored mechanisms for pattern formation in reaction-diffusion-advection (RDA) systems. A differential flow (different flow velocities of activator and inhibitor) was shown to have a similar destabilizing effect as differential diffusion (different rate of diffusion for different species) has in the Turing case [9–12].

On the other hand, a mechanism for the formation of steady patterns has been reported recently by Menzinger and co-workers, called flow-distributed oscillations (FDO) [13–15]. This apparently simple kinematic mechanism involves only advection (directional flow) and Hopf oscillations.

Flow-and-diffusion structures (FDS) appear as a generalization of the kinematic FDO mechanism to systems with differential flow and differential diffusion [13,16].

The importance of these mechanisms centers on the idea that growth, flow of cells, and gene oscillations are commonly present in a large number of biological processes during the first days of embryo development [8,17–19]. So the FDO and FDS mechanism may be a good candidate to explain some of the cell differentiation processes, as axial segmentation, skin patterning, or somitogenesis [20].

Some of the main theoretical characteristics for the FDS are as follows:

(i) FDS are steady patterns which are periodic in the direction of flow.

(ii) There is a lower limit value for the flow velocity, below which FDS patterns are not produced (absolute unstable regime) [21].

(iii) There is no upper limit for the formation of FDS in the convective unstable regime (that is, there is no upper limit for the flow velocity).

(iv) FDS can appear in systems with differential flow and differential diffusion.

(v) The wavelength is linearly dependent on the velocity of flow.

(vi) FDS are very robust, with a wide domain in the phase space, compared with other steady pattern formation systems, such as Turing patterns.

In this paper we present conclusive experimental verification of FDS patterns in a chemical medium. We use the similarity between a moving boundary and a boundary of advection (already used in Ref. [22]). A system with fixed domains and a boundary of advection is equivalent to a sufficiently large medium with a moving boundary, if it is observed from a reference frame co-moving with the boundary (in other words, the observer on top of a moving boundary sees an effective flow through it). Mathematically, both systems are identical when a change in the reference frame is introduced into the equations.

This equivalence allows us to perform experiments in a gel system without turbulence. Another advantage of having an effective flow created by the moving boundary, instead of a real flow, is that no hydrodynamical instability can distort the patterns, even in the case of high velocities.

We have used the photosensitive chlorine dioxide-iodine-malonic acid (CDIMA) reaction [23–25], where the difference between diffusion coefficients can be easily controlled chemically. In addition, light intensity can be used as a control parameter that allows transitions between the different regimes.

We have designed an experiment in which an oscillatory domain grows in a given direction with a well-controlled velocity. This is due to the displacement of a frontier separating an illuminated region from a shadowed domain (see Fig. 1). In this way, the role of the feeding boundary is played here by the moving boundary of illumination. Structures that are steady in the flow system are expected to move with the velocity of the boundary in the growing system. Owing to this equivalence, we shall present all results in the co-moving reference frame (unless specified) in order to maintain the analogy with the reaction-diffusion-advection

*Electronic address: miguez@brandeis.edu

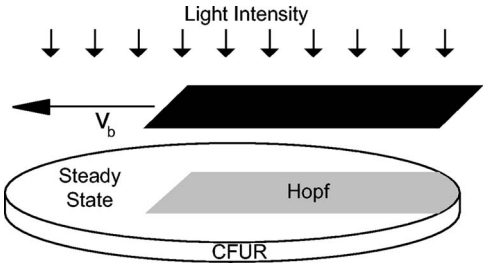

FIG. 1. Schematic of the experiment. The moving mask creates a growing shadow domain where structures can develop. Instead of the mask, a video projector was used, as described in the text.

system. Experiments were performed in a rectangular medium, where all the stationary boundaries were fixed by high light intensity, as illustrated in Fig. 1.

Experiments were carried out in a one-sided continuously fed unstirred tank reactor (CFUR) [26–28] maintained at (4±0.5 °C). Structures are formed in a circular agarose gel layer (2% agarose, thickness 0.3 mm, diameter 20 mm). Between the gel and the feeding chamber, we put an Anapore membrane (Whatman, pore size 0.2 mm, impregnated with 1% agarose) and a nitrocelulose membrane (Schleicher and Schuell, pore size 0.45 mm). The reagents of the CDIMA reaction were pumped into a continuously stirred tank reactor (CSTR) for mixing. Initial input concentrations in the CSTR were $[I_2]=0.45$ mM, [malonic acid]=1.1 mM, $[ClO_2]=0.18$ mM, $[H_2SO_4]=10$ mM, [PVA]=1 g/l.

Poly(vilyl)alcohol (PVA) is an indicator of the activator concentration, so it allows us to observe the patterns. PVA also reduces the diffusion coefficient of the activator with respect to the inhibitor. By changing the PVA concentration, we can vary the differential diffusion between activator and inhibitor, going from Hopf oscillations (low differential diffusion) to Turing patterns (high differential diffusion). For experimental purposes, the PVA concentration was set up to situate the system in oscillatory behavior, but with nonzero differential diffusion, matching the requirements for the FDS production.

The moving boundary was produced by focusing a moving image from a video projector (Hitachi, CP-X327) onto the gel. This allows us to impose a constant controlled velocity for the boundary of the decreasing illuminated zone (no pattern in the steady-state regime) at the expense of increasing the nonilluminated zone (allowing pattern formation in the oscillatory regime). Images were recorded by a charge-coupled device (CCD) camera.

Under these circumstances, the system exhibits phase waves of oscillation in the nonilluminated area. The period of oscillation is $T_o=0.74\pm0.05$ min and the spontaneous wavelength is $\lambda_o=1.22\pm0.08$ mm. In the illuminated area, the external light intensity is sufficiently high to situate the system in the steady-state regime.

In the absolute unstable regime, the pattern is composed of waves arising at the moving boundary and propagating in the opposite direction of the boundary velocity [see Fig. 2(a)]. In this space-time plot, the slope of the structures is the inverse of the velocity of the waves. As we increased the speed of the boundary, the phase waves slow down in

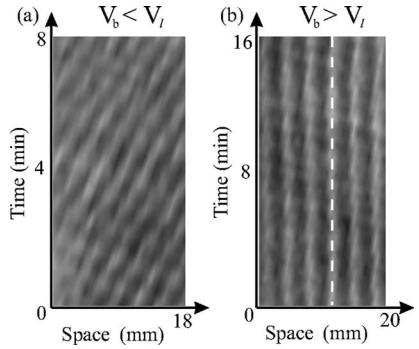

FIG. 2. Experimental space-time plot for different velocities of the boundary. The figure2 is a vertical array of experimental picture lines periodically taken (each line is recorded perpendicular to the moving boundary). Figures1 are shown in the reference frame comoving with the boundary. Note that the feeding boundary is always at space=0 mm. (a) velocity below FDS threshold ($V_b=1.02$ mm/min). (b) FDS ($V_b=7.09\pm0.92$ mm/min).

the moving reference frame. The period of forming a new wave ($T_0=0.74\pm0.05$ min) is independent of the boundary velocity.

If the velocity is increased, once the convective unstable regime is reached, waves became steady, forming a steady chemical structure that is spatially periodic in the direction of the velocity [see Fig. 2(b)]. Sometimes, a slow drift can be present leading to nonstrict steady patterns, maybe due to transient states. In general, the pattern remains steady, as can be observed comparing with the dashed vertical line in Fig. 2(b). In contrast to the case of lower velocities, the wavelength of the pattern, λ, is not fixed but depends on V_b via $\lambda=T_0V_b$. Figure 3 shows this linear dependence in solid agreement with the theoretical predictions [17]. These periodic patterns induced by the effective flow created by the moving boundary and reaction-diffusion are the theoretically predicted flow-and-diffusion structures [17,30]. As the theory predicts, increasing the value of the velocity shows the same behavior, and there is no upper limit for the velocity in which

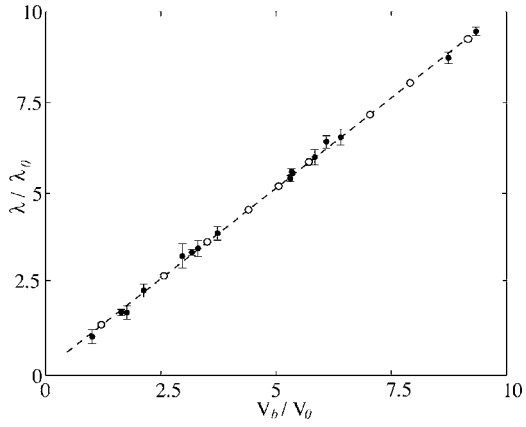

FIG. 3. Dependence of the wavelength of the FDS with the velocity of the boundary V_b. Wavelength and velocity are normalized in order to compare experimental results (represented by the ● symbol), where $\lambda_0=1.22\pm0.08$ mm, $V_0=1.64\pm0.08$ mm/min, numerical (○), and theoretical predictions (dashed line) $\lambda=T_0V_b$.

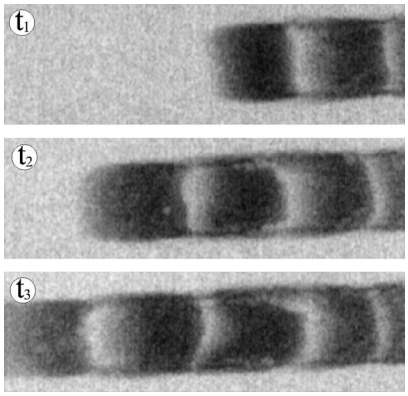

FIG. 4. Snapshots from the experiment corresponding to $V_b = 7.08 \pm 0.05$ mm/min. The photographs are shown in the laboratory reference frame. Size of each picture: 6×20 mm. Elapsed time between photographs: 0.75 min.

FDS will not form. FDS were found for a wide range of values in the parameter space. In fact, when the values of the parameters bring the system into the oscillatory domain, and the velocity of the moving boundary is larger than the velocity of normal autowaves, FDS are always produced.

The two-dimensional (2D) view of the experimental FDS in the laboratory reference frame is shown in Fig. 4. The spatial pattern is composed of stripes ordered parallel to the moving boundary. The stripes remain steady close to the boundary, where its influence is stronger. Far from the moving boundary (typically 7 or 8 wavelengths) the dynamic of the system is dominated by the Hopf instability, thus spontaneous oscillations and waves with V_0 and λ_0 occur. The study of the experimental two-dimensional FDS patterns is ongoing.

Numerical simulations have also been performed using the Lengyel-Epstein model for the CDIMA reaction [23,25,29]. Our model equations are

$$\partial_t u = a - cu - 4\frac{uv}{1+u^2} - \phi + \Delta u, \tag{1}$$

$$\partial_t v = \sigma\left(cu - \frac{uv}{1+u^2} + \phi + d\Delta v\right). \tag{2}$$

Here, u and v correspond to the the dimensionless concentrations of activator and inhibitor; a, c, and σ are dimensionless parameters proportional to other initial concentrations and rate constants, and d is the ratio of diffusion coefficients of inhibitor and activator. The value σ is proportional to the concentration of the PVA. The effect of external illumination is introduced through the ϕ terms. In this particular case, ϕ is in the form of a steplike function traveling through the medium with constant velocity V_b in the form: $\phi = \phi_0$ when $x < v_b t$ and $\phi = \phi_{max}$ when $x \geq v_b t$.

To mimic the experimental conditions, parameters for the simulations were set equal to $a=22$, $\sigma=5$, $c=1.3$, and $d=1.07$. $\phi_0=2$ corresponds to the low-light intensity case, with the solution of the system being inside the Hopf domain, whereas $\phi_{max}=4$ corresponds to the high-light intensity case, with the solution decaying to the steady state. A phase diagram is shown in Fig. 5.

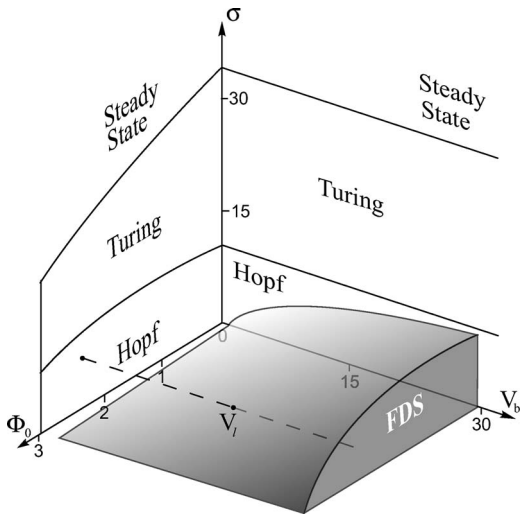

FIG. 5. Three-dimensional phase diagram for the L-E model with advection showing the different states for the parameters used. FDS are stable inside the gray domain. The threshold velocity can be identified as the surface of the gray area. Note that this threshold increases with the difference between the diffusion coefficients (proportional to σ). Dashed lines correspond to the numerical values chosen for the simulations.

In addition, to validate the analogy between the feeding and moving boundary, numerical simulations were performed using the same model but with a boundary of controlled and constant flow. We obtained identical results.

Figure 6 shows the numerical results obtained. In the absolute unstable regime, waves propagate backwards [Fig. 6(a)], while in the convective unstable regime, FDS appear stationary in the moving reference frame [Fig. 6(b)]. In Fig. 3 we also plot the dependence of λ vs V_b (in a dimensionless form) showing perfect agreement with the experiments and theory.

We have provided experimental evidence of the existence of flow-and-diffusion structures. The photosensitive CDIMA reaction in its oscillatory domain provides a good framework

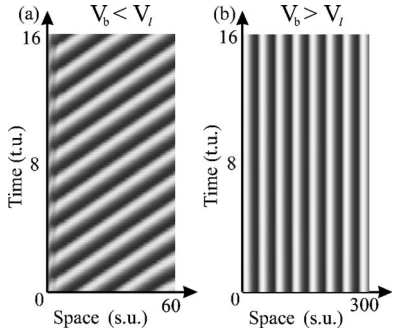

FIG. 6. Numerical space-time plot for different velocities of the boundary. Figure6s are shown in the comoving frame with the boundary. Note that the feeding boundary is always at space $=0$ mm. (a) Velocity below FDS threshold ($V_b=2$ s.u./t.u.). (b) FDS ($V_b=40$ s.u./t.u.).

of study, where differential diffusion can be chemically controlled. Due to the FDS mechanism, the effective flow generated by the moving boundary of illumination induces steady periodic patterns. Using a moving boundary of illumination we produce a growing oscillatory medium, thus ensuring no differential flow. The effective flow generates new phenomena through the FDS pattern formation mechanism. Structures formed are well controlled and considerably more robust than the classical reaction-diffusion patterns, which underscores the importance of this reaction-diffusion-advection mechanism in natural pattern forming processes.

Experiments were carried out in Santiago de Compostela with funding from the Spanish MCYT (Grant No. FIS2004-03006). We gratefully acknowledge the support from REACTOR and M. Menzinger, Irving R. Epstein, and L. Kramer for helpful discussions.

[1] A. M. Turing, Philos. Trans. R. Soc. London **327**, 31 (1952).
[2] J. D. Murray, *Mathematical Biology* (Springer-Verlag, Berlin, 1989).
[3] C. J. Koch and H. Meinhardt, Rev. Mod. Phys. **66**, 1481 (1994).
[4] H. Meinhardt, *The Algorithmic Beauty of Seashells* (Springer-Verlag, Berlin, 1998).
[5] B. N. Nagorcka and J. R. Mooney, J. Theor. Biol. **98**, 576 (1982).
[6] J. H. E. Cartwright, J. Theor. Biol. **217**, 97 (2002).
[7] M. Kærn, D. G. Míguez, A. P. Muñuzuri, and M. Menzinger, Biophys. Chem. **110**, 231 (2004).
[8] Mads Kaern, Michael Menzinger, Razvan Satnoianu, and Axel Hunding, Faraday Discuss. **120**, 295 (2001).
[9] A. B. Rovinsky and M. Menzinger, Phys. Rev. Lett. **70**, 778 (1993).
[10] R. A. Satnoianu, J. H. Merkin, and S. K. Scott, Dyn. Stab. Syst. **14**, 275 (1999).
[11] A. B. Rovinsky and M. Menzinger, Phys. Rev. Lett. **69**, 1193 (1992).
[12] R. Satnoianu and M. Menzinger, Phys. Lett. A **304**, 149 (2002).
[13] M. Kærn and M. Menzinger, Phys. Rev. E **60**, R3471 (1999).
[14] P. Andresén, M. Bache, E. Mosekilde, G. Dewel, and P. Borckmanns, Phys. Rev. E **60**, 297 (1999).
[15] M. Kærn and M. Menzinger, Phys. Rev. E **62**, 2994 (2000).
[16] R. A. Satnoianu, M. Menzinger, and P. K. Maini, J. Math. Biol. **41**, 493 (2000).
[17] R. A. Satnoianu, P. K. Maini, and M. Menzinger, Physica D **160**, 79 (2001).
[18] S. Schnell, K. J. Painter, P. K. Maini, and H. G. Othmer, *Volumes in Mathematics and its Applications* (Springer-Verlag, Berlin 2000), Vol. 121, p. 11.
[19] I. Palmeirim, D. Henrique, D. Ish-Horowicz, and O. Pourquié, Cell **91**, 639 (1997).
[20] M. Kærn, M. Menzinger, and A. Hunding, J. Theor. Biol. **2000**, 473 (2000).
[21] S. P. Kuznestov, E. Mosekilde, G. Dewel, and P. Borckmans, J. Chem. Phys. **106**, 7609 (1997).
[22] M. Kærn, R. Satnoianu, A. P. Muñuzuri, and M. Menzinger, Phys. Chem. Chem. Phys. **4**, 1319 (2002).
[23] I. Lengyel and I. R. Epstein, Science **251**, 650 (1991).
[24] B. Rudovics, E. Barillot, P. Davies, E. Dulos, J. Boissonade, and P. De Kepper, J. Phys. Chem. **103**, 1790 (1999).
[25] A. P. Muñuzuri, M. Dolnik, A. M. Zhabotinsky, and I. R. Epstein, J. Am. Chem. Soc. **121**, 8055 (1999).
[26] A. K. Horváth, M. Dolnik, A. P. Muñuzuri, A. M. Zhabotinsky, and I. R. Epstein, Phys. Rev. Lett. **83**, 2950 (1999).
[27] S. Rüdiger, D. G. Míguez, A. P. Muñuzuri, F. Sagués, and J. Casademunt, Phys. Rev. Lett. **90**, 128301 (2003).
[28] B. Peña, C. Pérez-García, A. Sanz-Anchelergues, D. G. Míguez, and A. P. Muñuzuri, Phys. Rev. E **68**, 056206 (2003).
[29] I. Lengyel, G. Rábai, and I. R. Epstein, J. Am. Chem. Soc. **112**, 9104 (1990).
[30] R. A. Satnoianu and M. Menzinger, Phys. Rev. E **62**, 113 (2000).